Optical model analysis of polarized neutron scattering from yttrium, lanthanum, and thulium

G. Schreder, W. Grum, J. W. Hammer, K.-W. Hoffmann, and G. Schleussner*
Institut für Strahlenphysik der Universität Stuttgart, 7000 Stuttgart 80, Federal Republic of Germany
(Received 28 September 1988)

Based on neutron differential cross section and analyzing power measurements at $E_n = 7.75$ MeV, optical-model parameters were deduced via spherical optical-model and coupled-channel calculations for the odd-even-nuclei ^{89}Y, ^{139}La, and ^{169}Tm. For the strongly deformed thulium ($\beta_2 = 0.31$), good fits to the sum of the angular distributions of the experimentally unresolved states could be achieved by coupling the ground-state rotational band.

I. INTRODUCTION

Angular distributions of neutron differential cross section and analyzing power of several nuclei have been measured at the Stuttgart SCORPION (Ref. 1) facility during the last few years. For the nuclei ^{89}Y, ^{139}La, and ^{169}Tm, the experimental results, together with their corresponding optical-model parameters at $E_n = 7.75$ MeV will be presented. Spherical optical-model (SOM) calculations were carried out for the nuclei yttrium and lanthanum, coupled-channel (CC) calculations were used for the strongly deformed nucleus thulium. In the case of yttrium it was possible to separate elastically from inelastically scattered neutrons, whereas for lanthanum with its first excited state at 166 keV the experimental resolution prevented the separation. Concerning thulium the situation was extreme: Within the range of the resolution there exists a couple of rotational bands. The assumption that only the ground-state rotational band contributes to the scattering process led to quite good fits to both our cross section and polarization data.

II. EXPERIMENTAL PROCEDURE

The scattering facility SCORPION and the experimental technique used have been presented in detail in Ref. 1. Neutrons of the ^{9}Be$(\alpha,n)^{12}$C-reaction were produced with the 500 μA currents of the Dynamitron accelerator with a polarization degree of 60% at 50° reaction angle.[2] The neutron flux at the scattering sample was 5×10^4 cm^{-2} s^{-1} using a beryllium layer of 1.2 μ deposited on a target-backing which was designed for high power dissipation.[1] The neutrons are collimated inside a spin precession magnet, which is switched in intervals of 5 min. The angular range for positioning the neutron detectors is $-124°$ to $+124°$. Neutron spectroscopy was performed by using NE-213 scintillation counters and unfolding of the proton recoil spectra with the improved Ferdor-code FANTI.[1] The contribution of γ events could be kept below typically 1% by means of sophisticated n-γ-discrimination circuits.[1] The overall energy resolution (detectors and unfolding procedure) was about 800 keV. Four scintillation detectors were installed to monitor the neutron flux at the target and at the sample position during long foreground and background runs. Background runs were performed with the sample in position and by closing the collimators of the detectors with rods of copper (15 cm) and polyethylene (60 cm). The calibration of the setup to absolute cross section values was performed by normalization to the hydrogen cross section using a polyethylene sample. To arrive at sufficient counting statistics of the scattered events a minimal sample size is required, which was not available for thulium. The properties of the samples used for this experiment are listed in Table I. The data for lanthanum were corrected for scattering contributions from its steel containment.

III. DATA EVALUATION AND RESULTS

After unfolding the proton recoil scintillation spectra the relative angular distributions were obtained. An important step of data evaluation is the finite geometry correction including corrections due to flux attenuation

TABLE I. Properties of the scattering samples.

Element	Size (mm)	Abundance (%)	Weight (g)	Nuclei ($\times10^{23}$)
^{89}Y	50.15×40.25 Ø	100.000	285.20	19.32
^{139}La[a]	49.60×39.40 Ø	99.911	366.10	15.73
^{169}Tm	30.00×19.20 Ø	100.000	76.70	2.71
PE	40.00×30.00 Ø		26.37	22.48

[a]Steel cylinder (wall 0.3 mm in thickness).

and depolarization in the scattering sample. In the first step the experimental differential cross section angular distribution was raised by a normalization factor due to an estimate of the overall flux attenuation, which was obtained using Kinney's method.[3] The distribution corrected in this way was used as input for an extended version of the Monte Carlo code JANE.[4,5] JANE was modified to calculate also flux attenuation (XJANE).[6] The contributions of single and double scattering were calculated, and the next iteration was based on these results, as did an estimate for triple scattering. Within the quoted range of errors this procedure led to consistent angular distributions, which will be referred to as *experimental data* in the following text. They are given in Figs. 1–3. Tables are available from the authors.

IV. OPTICAL MODEL ANALYSIS

Upper limits for compound scattering contributions were estimated with the code[7] CERBERO3. They were found to be negligible, as the level densities are already high enough at our excitation energy of 7.75 MeV. Required data were taken from Refs. 8–12, 13–16, and 17–19 for Y, La, and Tm, respectively. The usual complex optical-model potential in the presented energy range—including a central real, a surface imaginary, and a complex spin-orbit interaction—is of the form

$$U(r) = -V_R f_R(r) + 4ia_D W_D g_D(r) + \lambda\!\!\!^{-2}_{\pi}(V_{SO} + iW_{SO})\frac{1}{r}g_{SO}(r)(2\mathbf{l}\cdot\mathbf{s}) , \quad (1)$$

$$\lambda\!\!\!^{-}_{\pi} = \frac{\hbar}{m_\pi c} \cdots \text{pion compton wavelength} .$$

with the Woods-Saxon form factors

$$f_X(r) = \frac{1}{1+\exp[(r-R_X)/a_X]} \quad (2)$$

and

$$g_X(r) = \frac{df_X}{dr} = \frac{1}{a_X} f_X(f_X - 1) ,$$

with $X = R$, D, and SO. The nuclear radius is given by $R \equiv R_0 = r_0 A^{1/3}$ for spherical nuclei. In the case of deformed nuclei the radius is expressed by an expansion in spherical harmonics. The deviation from spherical symmetry introduces a coupling of the Schrödinger equations for different scattering channels.[20] The model is able to describe rotational as well as vibrational excitations of a nucleus. The calculations were carried out with the code[21] ECIS79. The absolute normalization of the differential cross section was used as an additional parameter in the search.

A. Yttrium

The first excited $g_{9/2}$ state can be explained by an excitation of the single unpaired proton in the shell model.[22,23] Therefore only the ground state was included in the calculations. To start the parameter search the global set of Delaroche *et al.*[24] for neutron differential cross section data was taken. The result for the spherical optical model (SOM) provides an excellent description of the measured angular distributions, as can be seen in Fig. 1. The coupling of a $L = 5^-$ phonon to the 0^+ ground state of the strontium core in order to describe the first excited state was not convincing. The introduction of an imaginary spin-orbit potential[25] drastically reduces the χ^2 for the analyzing power. Only the depth W_{SO} was searched independently, the geometry was kept the same as for the real potential. The calculations revealed a reasonable value of about 0.4 MeV with the same sign as the real part. Although our neutron energy lies slightly below the cited range of validity ($7.9 \leq E_n \leq 16.9$ MeV) for the Triangle Universities Nuclear Laboratory (TUNL) parameters of Ref. 25, these are consistent with the analyzing power data of the present work, too. The parameter sets are compared in Table II.

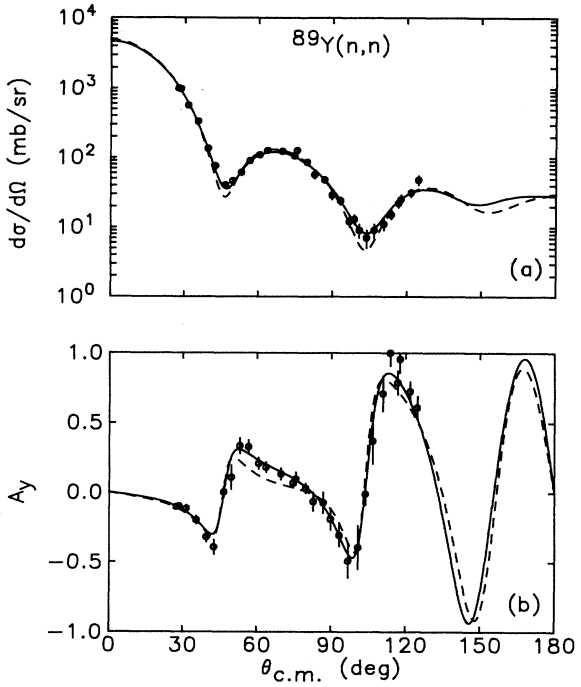

FIG. 1. Differential cross section and analyzing power angular distributions for yttrium. The data are given together with the optical-model results of the present work (solid line). The dashed curves were calculated with the TUNL parameters.

B. Lanthanum

The correction for scattering events in the steel containment was carried out with cross section data for ^{56}Fe from Ref. 28 and polarization data for natural iron measured at SCORPION.[29] It turned out that the analyzing power distribution remained nearly unchanged, whereas in the first minimum of the differential cross section the corrections were large. The first two states of lanthanum can be described by the shell model. The rather small quadrupole moment suggests that the nucleus is of spher-

TABLE II. Neutron optical-model parameters at $E_n = 7.75$ MeV.

Parameter	^{89}Y This work	^{89}Y TUNL[a]	^{139}La	^{169}Tm $0^+-2^+-4^+$
V_R (MeV)	45.90	49.31	44.44	45.39
r_R (fm)	1.25	1.20	1.25	1.28
a_R (fm)	0.65	0.69	0.65	0.49
J/A (MeV fm^3)[b]	425.2	414.8	399.2	417.5
$\langle r^2\rangle^{1/2}$ (fm)[b]	4.947	4.872	5.558	5.774
W_D (MeV)	6.59	7.29	6.74	7.91
r_D (fm)	1.29	1.31	1.33	1.16
a_D (fm)	0.51	0.50	0.46	0.58
J/A (MeV fm^3)[b]	64.5	72.1	54.0	57.6
$\langle r^2\rangle^{1/2}$ (fm)[b]	6.115	6.186	7.134	6.821
V_{SO} (MeV)	7.95	6.58	6.90	5.22
r_{SO} (fm)	1.19	1.14	1.11	1.11
a_{SO} (fm)	0.54	0.50	0.47	0.31
$J/A^{1/3}$ (MeV fm)[b]	237.5	188.3	192.3	145.5
$\langle r^2\rangle^{1/2}$ (fm)[b]	5.575	5.325	5.935	6.213
W_{SO} (MeV)	0.70	0.67	0.92	−0.28
r_{SO} (fm)	1.19	1.26	1.11	1.11
a_{SO} (fm)	0.54	0.50	0.47	0.31
$J/A^{1/3}$ (MeV fm)[b]	20.9	21.2	25.6	−7.8
$\langle r^2\rangle^{1/2}$ (fm)[b]	5.575	5.838	5.935	6.213
renormalized$_\sigma$	0.96	0.86	0.95	0.89
χ^2_σ (N)	32 (31)	70 (31)	24 (36)	20 (30)
χ^2_A (N)	23 (30)	63 (30)	34 (38)	32 (29)
σ_{cal} (mb)	4296	4140	4477	5312[c]
σ_{exp} (mb)	4300±100[d]		4300±90[e]	~5150[d]

[a]Reference 25.
[b]See Appendix.
[c]Direct channels included (2^+:279 mb; 4^+: 90 mb).
[d]Reference 26.
[e]Reference 27.

ical shape, the $\frac{7}{2}^+$ g.s. and the $\frac{5}{2}^+$ excited state being explained by states of the single unpaired proton.[30,31] Therefore the unresolved scattering to the $\frac{5}{2}^+$ state is supposed to be negligible. Figure 2 shows that the data are quite well reproduced by the SOM, parameters are given in Table II.

C. Thulium

Thulium is a typical example for a strongly deformed nucleus with a $K = \frac{1}{2}^+$ g.s. rotational band.[32] The rich band structure[17] in the excitation energy range up to 600 keV is unresolvable by our neutron spectroscopy. As admixtures of further $K = \frac{3}{2}^+$ bands are not too strong,[33] our CC calculations included the g.s. rotational band alone. Due to restrictions on computing time the fictitious coupling scheme $0^+-2^+-4^+$ of Table III was applied. The moment of inertia of the actual nucleus is used for obtaining the excited states of the fictitious even-even nucleus.[34] The optical-model parameters are given in Table II. The superposition of elastic and inelastic scattering introduces an extreme ambiguity concerning the central imaginary potential. Figure 3 shows experimental and model distributions.

TABLE III. Identifications of ^{169}Tm—levels and the corresponding fictitious band.

Tm levels keV	Tm levels I^π	Fictitious levels keV	Fictitious levels I^π
0.0	$\frac{1}{2}^+$	0.0	0^+
8.4	$\frac{3}{2}^+$	72.0	2^+
118.2	$\frac{5}{2}^+$		
138.9	$\frac{7}{2}^+$	240.0	4^+
332.0	$\frac{9}{2}^+$		
367.4	$\frac{11}{2}^+$	510.0	6^+
636.8	$\frac{13}{2}^+$		

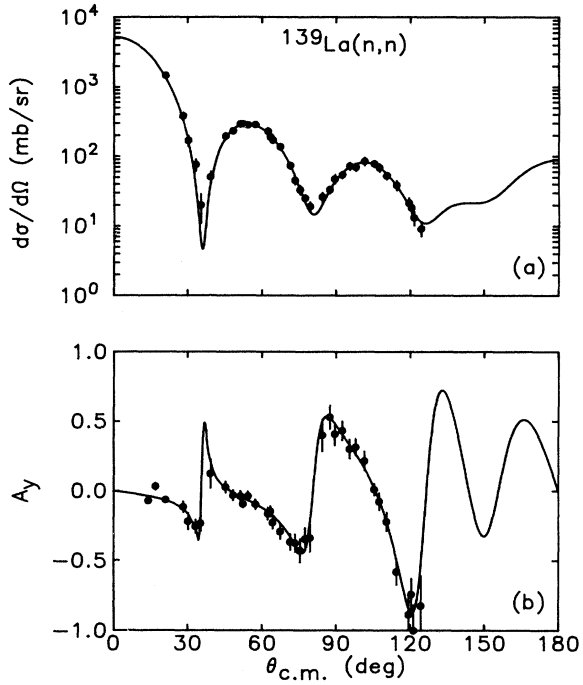

FIG. 2. Differential cross section and analyzing power angular distributions for lanthanum. The experimental data points are given together with the optical-model results.

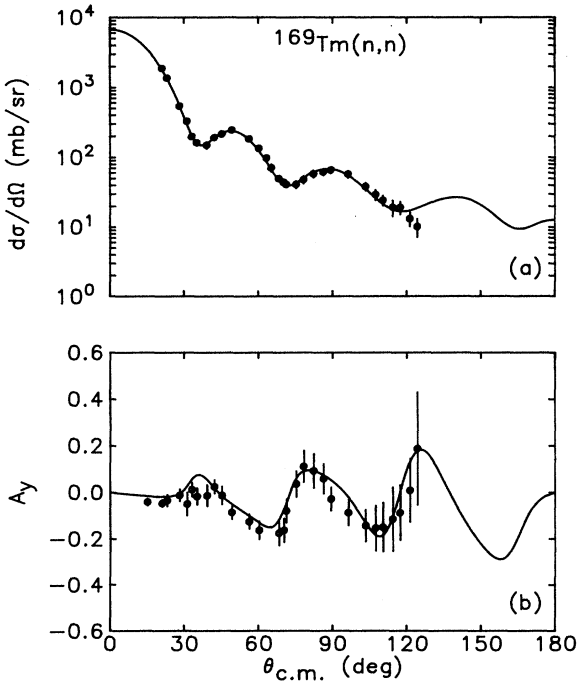

FIG. 3. Differential cross section and analyzing power angular distributions for thulium. The experimental data points are given together with the coupled-channel results.

V. CONCLUSION

It has been shown that polarized neutron scattering at 7.75 MeV is well described by SOM calculations for yttrium and lanthanum, and by CC calculations for thulium, producing reasonable parameters. The coupling of further states or bands to the ground-state band of thulium does not seem meaningful unless some inelastic channels can be resolved by experiment. It is for the same reason that a determination of the imaginary spin-orbit potential should be taken with care, whereas for yttrium and lanthanum the values of $J_{W_{SO}}/A^{1/3}$ suggest a smooth behavior over the medium mass range. Compared to the real central part the smaller radius parameter of the spin-orbit interaction is a common characteristic of the parameter sets (Table II).

ACKNOWLEDGMENTS

The authors wish to thank the accelerator staff (B. Fischer, H. Hollick, F. Kutz, and J. Lefèvre) for the provision of high-beam currents as the base of the experimental part of this work. M. Mattes (Institut für Kernenergetik und Energiesysteme Stuttgart) provided us with the most recent neutron data. Further gratitude is expressed to G. Haouat [Centre d'Etudes Nucleaires (CEN) Bruyères-le-Châtel] for lending us the thulium sample. We are also indebted to J. Raynal (CEN Saclay) for the provision of his code ECIS79.

APPENDIX

The intercomparison of various optical potentials essentially involves their volume integrals and mean-square radii. For the widely used Woods-Saxon (WS) and quadratic WS form factors analytic expressions will be listed below. They can easily be extended to higher potences of the WS form.

The volume integral and the mean-square radius are defined by

$$\frac{J}{A}=\left[\frac{1}{A}\right]\int V(\mathbf{r})d\tau$$

and (A1)

$$\langle R^2\rangle=\frac{\int V(\mathbf{r})r^2 d\tau}{\int V(\mathbf{r})d\tau}\ .$$

For the evaluation of the integral

$$F_n(k)=\int_0^\infty \frac{x^n dx}{1+e^{x-k}} \quad \text{(A2)}$$

we follow the way of Elton,[35] who obtains

$$F_n(k)=\frac{k^{n+1}}{n+1}-\sum_{m=1}^{\infty}\frac{(-1)^m}{m}\left\{\sum_{r=0}^{n}[1-(-1)^r]\frac{n!}{m^r(n-r)!}k^{n-r}+\frac{(-1)^n n!}{m^n}e^{-mk}\right\}. \tag{A3}$$

The last sum is neglected, its largest term being $0(e^{-k})$. Thus

$$F_0(k)=k\ , \tag{A4}$$

$$F_1(k)=\frac{k^2}{2}+\frac{\pi^2}{6}\ , \tag{A5}$$

$$F_2(k)=\frac{k^3}{3}+\frac{\pi^2 k}{3}\ , \tag{A6}$$

$$F_3(k)=\frac{k^4}{4}+\frac{\pi^2 k^2}{2}+\frac{7\pi^4}{60}\ , \tag{A7}$$

$$F_4(k)=\frac{k^5}{5}+\frac{2\pi^2 k^3}{3}+\frac{7\pi^4 k}{15}\ . \tag{A8}$$

The usual parametrization of WS volume, WS derivative, and WS spin-orbit yields:

WS volume:

$$J_V=4\pi V a^3 F_2\left[\frac{R}{a}\right],\quad \langle R^2\rangle_V=a^2\frac{F_4\left[\frac{R}{a}\right]}{F_2\left[\frac{R}{a}\right]}\ , \tag{A9}$$

which gives (Ref. 36)

$$\left[\frac{J}{A}\right]_V=\frac{4\pi}{3}r^3 V\left[1+\left[\frac{\pi a}{R}\right]^2\right],\qquad \langle R^2\rangle_V=\tfrac{1}{5}(3R^2+7\pi^2 a^2)\ . \tag{A10}$$

WS derivative:

$$J_W=4\pi(-4aW)(-2a^2)F_1\left[\frac{R}{a}\right], \tag{A11}$$

$$\langle R^2\rangle_W=2a^2\frac{F_3\left[\frac{R}{a}\right]}{F_1\left[\frac{R}{a}\right]}\ ,$$

which gives

$$\left[\frac{J}{A}\right]_W=16\frac{\pi R^2}{A}aW\left[1+\frac{1}{3}\left[\frac{\pi a}{R}\right]^2\right]\ \text{(Ref. 36)}\ , \tag{A12}$$

$$\langle R^2\rangle_W=3R^2\frac{1+2\left[\frac{\pi a}{R}\right]^2+\frac{7}{15}\left[\frac{\pi a}{R}\right]^4}{3+\left[\frac{\pi a}{R}\right]^2}\ . \tag{A13}$$

WS spin-orbit:

$$J_{SO}=4\pi(-2V_{SO})(-a)F_0\left[\frac{R}{a}\right],$$

$$\langle R^2\rangle_{SO}=3a^2\frac{F_2\left[\frac{R}{a}\right]}{F_0\left[\frac{R}{a}\right]}\ , \tag{A14}$$

which gives (Ref. 37)

$$\left[\frac{J}{A^{1/3}}\right]_{SO}=8\pi r V_{SO}\ \text{and}\ \langle R^2\rangle_{SO}=R^2\left[1+\left[\frac{\pi a}{R}\right]^2\right]. \tag{A15}$$

Quadratic WS:

For the evaluation of the integral

$$G_n(k)=\int_0^{\infty}x^n f^2(x)dx\ \text{with}\ f(x)=\frac{1}{1+e^{x-k}} \tag{A16}$$

we make use of the identity

$$\frac{\partial f(x)}{\partial x}=f^2(x)-f(x)\ , \tag{A17}$$

thus obtaining

$$G_n(k)=[x^n f]_0^{\infty}+F_n(k)-nF_{n-1}(k)\ , \tag{A18}$$

and for the derivative form factors

$$\int_0^{\infty}x^n\frac{\partial}{\partial x}[f^2(x)]dx=[x^n f^2]_0^{\infty}-nG_{n-1}(k)\ . \tag{A19}$$

The application of the above scheme for higher potences of the WS form factor is straightforward.

*Deceased.

[1]J. W. Hammer, G. Bulski, W. Grum, W. Kratschmer, H. Postner, and G. Schleussner, Nucl. Instrum. Methods **244**, 455 (1986).

[2]W. Weiss, Nucl. Instrum. Methods (to be published).

[3]W. E. Kinney, Nucl. Instrum. Methods. **83**, 15 (1970).

[4]E. Woye, code JANE, private communication.

[5]E. Woye, W. Tornow, G. Mack, C. E. Floyd, P. P. Guss, K. Murphy, R. C. Byrd, S. A. Wender, R. L. Walter, T. B. Clegg, and W. Wylie, Nucl. Phys. **A394**, 139 (1983).

[6]W. Grum, code XJANE (unpublished).

[7]F. Fabbri, G. Fratamico, and G. Reffo, code CERBERO3 (Nu-

clear Energy Agency Data Bank, Gif-sur-Yvette, 1977).
[8]E. D. Arthur, Nucl. Sci. Eng. **76**, 137 (1980).
[9]G. Nardelli, and G. Tornielli, Nuovo Cimento **94A**, 196 (1986).
[10]D. C. Kocher, Nucl. Data Sheets **16**, 445 (1975).
[11]D. C. Kocher, Nucl. Data Sheets **16**, 55 (1975).
[12]J. W. Tepel, Nucl. Data Sheets **25**, 553 (1978).
[13]W. Dilg, W. Schantl, H. Vonach, and M. Uhl, Nucl. Phys. **A217**, 269 (1973).
[14]L. K. Peker, Nucl. Data Sheets **32**, 1 (1981).
[15]T. W. Burrows, Nucl. Data Sheets **52**, 273 (1987).
[16]L. K. Peker, Nucl. Data Sheets **51**, 395 (1987).
[17]V. S. Shirley, Nucl. Data Sheets **36**, 443 (1982).
[18]A. E. Ignatochkin, E. N. Shurshikov, and Yu. F. Jaborov, Nucl. Data Sheets **52**, 365 (1987).
[19]Zhou Chunmei, Nucl. Data Sheets **50**, 351 (1987).
[20]T. Tamura, Rev. Mod. Phys. **37**, 679 (1965).
[21]J. Raynal, coupled-channel code ECIS79 (Nuclear Energy Agency Data Bank, Gif-sur-Yvette, 1979).
[22]O. Schwentker, J. Dawson, S. McCaffrey, J. Robb, J. Heisenberg, J. Lichtenstadt, C. N. Papanicolas, J. Wise, J. S. McCarthy, N. Hintz, and H. P. Blok, Phys. Lett. **112B**, 40 (1982).
[23]O. Schwentker, J. Dawson, J. Robb, J. Heisenberg, J. Lichtenstadt, C. N. Papanicolas, J. Wise, J. S. McCarthy, L. T. van der Bijl, and H. P. Blok, Phys. Rev. Lett. **50**, 15 (1983).
[24]J. P. Delaroche, Ch. Lagrange, and J. Salvy, in *Proceedings of a Consultants Meeting on the Use of Nuclear Theory in Neutron Nuclear Data Evaluation, Trieste, 1975* (IAEA-190, Vol. 1, Vienna, 1976).
[25]G. M. Honoré, R. S. Pedroni, C. R. Howell, H. G. Pfützner, R. C. Byrd, G. Tungate, and R. L. Walter, Phys. Rev. C **34**, 825 (1986).
[26]D. G. Foster, Jr. and D. W. Glasgow, Phys. Rev. C **3**, 576 (1971).
[27]H. S. Camarda, T. W. Phillips, and R. M. White, Phys. Rev. C **29**, 2106 (1984).
[28]S. M. El-Kadi, C. E. Nelson, F. O. Purser, R. L. Walter, A. Beyerle, C. R. Gould, and L. W. Seagondollar, Nucl. Phys. **A390**, 509 (1982).
[29]G. Schreder *et al.* (unpublished).
[30]R. G. Kulkarni and K. Andhradev, Can. J. Phys. **57**, 1940 (1979).
[31]S. H. Faller, C. A. Stone, J. D. Robertson, Chien Chung, N. K. Aras, W. B. Walters, R. L. Gill, and A. Piotrowski, Phys. Rev. C **34**, 654 (1986).
[32]P. G. Young, E. D. Arthur, C. Philis, P. Nagel, and M. Collin, in *Proceedings of the International Conference on Nuclear Data for Science and Technology, Antwerp, 1982,* edited by K. H. Böckhoff (Reidel, Dordrecht, 1982).
[33]P. Taras, D. Ward, H. R. Andrews, J. S. Geiger, R. L. Graham, and W. McLatchie, Nucl. Phys. **A289**, 165 (1977).
[34]Ch. Lagrange, O. Bersillon, and D. G. Madland, Nucl. Sci. Eng. **83**, 396 (1983).
[35]L. R. B. Elton, Nucl. Phys. **5**, 173 (1958).
[36]J. Rapaport, V. Kulkarni, and R. W. Finlay, Nucl. Phys. **A330**, 15 (1979).
[37]F. A. Brieva and J. R. Rook, Nucl. Phys. **A297**, 206 (1978).